# Merging GPS and Atmospherically Corrected InSAR Data to Map 3-D Terrain Displacement Velocity

João Catalão, *Member, IEEE*, Giovanni Nico, *Senior Member, IEEE*, Ramon Hanssen, and Cristina Catita

*Abstract*—A method to derive accurate spatially dense maps of 3-D terrain displacement velocity is presented. It is based on the merging of terrain displacement velocities estimated by time series of interferometric synthetic aperture radar (InSAR) data acquired along ascending and descending orbits and repeated GPS measurements. The method uses selected persistent scatterers (PSs) and GPS measurements of the horizontal velocity. An important step of the proposed method is the mitigation of the impact of atmospheric phase delay in InSAR data. It is shown that accurate vertical velocities at PS locations can be retrieved if smooth horizontal velocity variations can be assumed. Furthermore, the mitigation of atmospheric effects reduces the spatial dispersion of vertical velocity estimates resulting in a more spatially regular 3-D velocity map. The proposed methodology is applied to the case study of Azores islands characterized by important tectonic phenomena.

*Index Terms*—Atmospheric phase delay, GPS, SAR interferometry (InSAR), synthetic aperture radar (SAR), tectonics.

## I. INTRODUCTION

INTERFEROMETRIC synthetic aperture radar (InSAR) techniques have proved their potential in a large number of applications (see, for example, [1], [2], and references therein). In particular, spaceborne InSAR provides high-resolution maps of crust displacement over wide areas [3], [4]. The accuracy of displacement measurements is in the order of a fraction of the radar wavelength, and the sampling period ranges from 11 days (TerraSAR-X and Cosmo-Sky-Med) to about 24–46 days [Radarsat, Environmental Satellite (ENVISAT)-Advanced Synthetic Aperture Radar (ASAR), Advanced Land Observation Satellite-Phased Array type L-band Synthetic Aperture Radar). These measurements are well documented in the studies of geophysical phenomena such as earthquakes [5], [6], subsidence [7] and bradyseism [8], landslides [9], and volcanoes

J. Catalão and C. Catita are with the Instituto Dom Luís, Universidade de Lisboa, 1269-102 Lisboa, Portugal.

G. Nico is with the Istituto per le Applicazioni del Calcolo, Consiglio Nazionale delle Ricerche (CNR-IAC), 70126 Bari, Italy (e-mail: g.nico@ba.iac.cnr.it).

R. Hanssen is with Delft University of Technology, 2600 AA Delft, The Netherlands.

Color versions of one or more of the figures in this paper are available online at http://ieeexplore.ieee.org.

[10]. However, the InSAR technique has two limitations. First, it measures only one component of the 3-D terrain displacement, along the radar line of sight (LOS). This means that a single InSAR measurement does not allow to derive the 3-D surface displacement. Second, the InSAR measurement contains information on both terrain displacement and temporal changes of atmospheric phase delay and needs a means to disentangle geodetic and atmospheric signals. As far as the first limitation is concerned, it is worth mentioning that 3-D terrain displacement is difficult to measure even in the case of InSAR measurements taken along both ascending and descending satellite passes. In fact, even in this case, there would be three unknown velocity components and just two independent InSAR LOS velocity measurements. For that, methodologies have been proposed in the literature for the merging of InSAR and repeated GPS measurements [11], [12]. Gudmundsson and Sigmundsson described a method based on Markov random field regularization and simulated annealing [11]. The method requires unwrapped interferograms and repeated GPS measurements of terrain velocity as inputs. The GPS observations are interpolated on the InSAR grid, and a 3-D velocity value is assigned to each pixel of interferograms. These values are used as a first guess map of 3-D terrain velocity which is then updated by means of a Bayesian statistical approach which minimizes an energy function depending on the difference between InSAR and GPS measurements at pixel level and on its spatial regularity. As many Bayesian approaches require a global optimization technique, this method has the disadvantage of slow convergence to the final solution and its strong dependence on the initial condition. Samsonov and Tiampo proposed a simple merging strategy using analytical optimization [12]. They reconstructed a 3-D velocity map by using sparse GPS measurements and two differential interferograms taken along ascending and descending satellite passes. Both the aforementioned methods demonstrated the improvement of the accuracy of velocity maps derived from GPS data alone also due to the spatial continuity of velocity information contained in SAR interferograms. Unfortunately, many real applications are faced with the problem of low coherence interferograms. In such cases, there is a need to process the time series of interferograms acquired over the same area using advanced InSAR techniques. Generally, the outcome of this processing is the estimation of terrain velocity in just a few selected points characterized by good quality interferometric phase. In this case, the problem we are facing is the comparison between two sets of sparse measurements, namely, the InSAR one, generally having a higher spatial density, and the set of GPS measurements. As far as the second limitation is concerned,

a method was presented to mitigate the atmospheric phase artifacts in SAR interferograms based on the interpolation of zenith wet delay data obtained from a network of GPS receivers in the region imaged by the radar [13]. Another approach to mitigate the spatiotemporal variations of InSAR phase due to radar signal propagation in the atmosphere is based on near-infrared water vapor data (e.g., acquired by the National Aeronautics and Space Administration Moderate Resolution Imaging SpectroRadiometer or the European Space Agency MEdium Resolution Imaging Spectrometer) [14]. Unfortunately, this approach is sensitive to the presence of clouds over the study region. A promising way to disentangle geodetic and atmospheric signals in InSAR data relies on forecasts produced by high-resolution numerical weather models. For instance, Foster *et al.* used the National Center for Atmospheric Research–Penn State Mesoscale Model Version 5 to produce predictions of atmospheric temperature and pressure and water vapor fields at a 3-km horizontal resolution. For any SAR image acquisition, they computed the 3-D refractivity field and radar phase delay [15]. A similar approach was adopted by Nico *et al.* [16] using the high-resolution Weather Research and Forecasting (WRF) model to generate forecasts of the atmospheric parameters at a 1-km horizontal resolution and at the same time of SAR acquisitions. It has been proven that forecasts based on numerical weather models can mitigate phase variance due to atmospheric artifacts [15], [16].

In this paper, we describe a methodology to derive accurate maps of 3-D terrain displacement based on the merging of InSAR point-like estimations and repeated GPS measurements of terrain displacement velocity. Time series of SAR interferograms acquired along ascending and descending satellite orbits are processed to identify terrain patches acting as persistent scatterers (PS). The technique introduced by Hooper *et al.* [17] was chosen to process SAR data since it is more suitable to estimate terrain displacements in nonurban areas which are those generally characterized by low coherence conditions. The impact of atmospheric artifact mitigation on displacement map accuracy is also studied by comparing the variance of terrain displacement velocities at the PS located close to each GPS station before and after the mitigation of atmospheric effects modeled by using WRF forecasts [16]. The structure of the paper is as follows. Section II describes the methodology to merge GPS and PS-InSAR estimates to derive a map of the 3-D terrain displacement velocities. Section III presents the velocity maps obtained by means of repeated GPS measurements. The processing of InSAR data and the mitigation of atmospheric effects are discussed in Section IV. Results of data merging and assessment of velocity map are given in Section V. Finally, a few conclusions are drawn in Section VI.

## II. METHODOLOGY

The outcome of PS-InSAR processing is an estimation of terrain displacement velocity in a set of terrain patches able to generate PS. However, this technique can only measure the LOS component of terrain displacement. More information on 3-D displacement velocity is difficult to extract even when ascending and descending InSAR time series are available. The
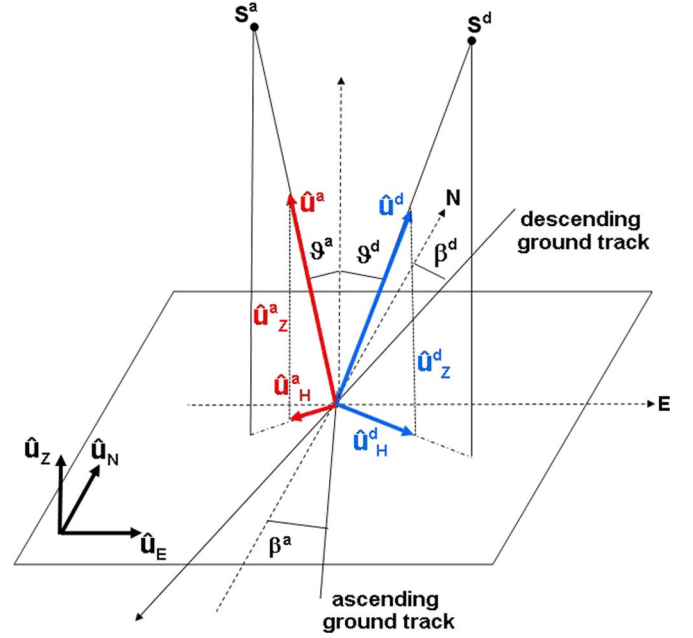


Fig. 1. Sketch with the geometry of ascending and descending InSAR geometries with unit vectors (red) $\mathbf{u^a}$ and (blue) $\mathbf{u^d}$, radar incidence angles $\vartheta_a$ and $\vartheta_d$, and angles $\beta^a$ and $\beta^d$ related to ground-track azimuthal angles. The horizontal components of unit vectors $\mathbf{u^a}$ and $\mathbf{u^d}$ are also depicted. For the sake of clarity, the common vertical components of unit vectors are omitted.

methodology we present try to solve this problem by merging PS and GPS measurements. The GPS technique provides more precise measurements of the horizontal than the vertical velocity. In contrast, the PS-InSAR technique is more sensitive to the vertical than the horizontal velocity. The idea of this paper is to derive the 3-D terrain displacement velocity by merging measurements of the horizontal velocity provided by GPS and of the PS velocities. Let us introduce the unit vectors $\mathbf{u^a} = \{u_E^a, u_N^a, u_Z^a\}$ and $\mathbf{u^d} = \{u_E^d, u_N^d, u_Z^d\}$, pointing from PS to the satellite moving along, respectively, the ascending and descending orbits. Fig. 1 shows a sketch of an InSAR configuration with both ascending and descending orbits. The components of unit vectors $\mathbf{u}$ ($\mathbf{u^a}$ or $\mathbf{u^d}$), respectively, along the West–East, South–North, and vertical directions, are given in terms of the local radar incidence angles $\vartheta$ ($\vartheta^a$ or $\vartheta^d$) and ground-track azimuthal angles $\alpha$ ($\alpha^a$ or $\alpha^d$) as

$$\begin{cases} u_E = \sin\vartheta \sin\left(\alpha - \frac{\pi}{2}\right) \\ u_N = \sin\vartheta \cos\left(\alpha - \frac{\pi}{2}\right) \\ u_Z = \cos\vartheta \end{cases} \quad (1)$$

where $\alpha^a = -\beta^a$ and $\alpha^d = \beta^d + \pi$, with $\beta$ ($\beta^a$ or $\beta^d$) being the smaller angles between the South–North and ground-track directions (see Fig. 1). The three components of the terrain displacement velocity $\mathbf{v} = \{v_E, v_N, v_Z\}$ can be estimated by minimizing the following energy function:

$$E = \sum_{i\in\{a,d\}} \left(v_{PS}^i - u_E^i v_E - u_N^i v_N - u_Z^i v_Z\right)^2 \quad (2)$$

where $v_{PS}^a$ and $v_{PS}^d$ are the PS-InSAR LOS velocities estimated along the ascending and descending orbits. The minimum value

of the cost function $E$ is reached when its first derivatives with respect to each component of the unknown terrain displacement velocity $\mathbf{v}$ are zero. This gives rise to the following linear equation $\mathbf{M} \cdot \mathbf{v} = \mathbf{a}$, i.e.,

$$\begin{bmatrix} u_E^{a2} + u_E^{d2} & u_E^a u_N^a + u_E^d u_N^d & u_E^a u_Z^a + u_E^d u_Z^d \\ u_N^a u_E^a + u_N^d u_E^d & u_N^{a2} + u_N^{d2} & u_N^a u_Z^a + u_N^d u_Z^d \\ u_Z^a u_E^a + u_Z^d u_E^d & u_Z^a u_N^a + u_Z^d u_N^d & u_Z^{a2} + u_Z^{a2} \end{bmatrix}$$
$$\cdot \begin{bmatrix} v_E \\ v_N \\ v_Z \end{bmatrix} = \begin{bmatrix} u_E^a v_{PS}^a + u_E^d v_{PS}^d \\ u_N^a v_{PS}^a + u_N^d v_{PS}^d \\ u_Z^a v_{PS}^a + u_Z^d v_{PS}^d \end{bmatrix}. \quad (3)$$

The matrix $\mathbf{M}$ in (3) depends only on InSAR configuration geometry. It is ill-conditioned for the values of look and track angle typical of all current spaceborne SAR missions, thus making its inversion difficult.

To avoid this problem, we propose a simple methodology to extract the components of vector $\mathbf{v}$ from the ascending and descending InSAR time series, based on the availability of repeated GPS measurements in a few sparse points. The LOS velocities $\mathbf{v}_{PS}$ ($\mathbf{v}_{PS}^a$ or $\mathbf{v}_{PS}^d$) estimated by PS-InSAR are decomposed into horizontal and vertical components as follows:

$$\mathbf{v}_{PS} = v_{PS}^{(H)} \cdot \mathbf{u}_H + v_{PS}^{(Z)} \cdot \mathbf{u}_Z \quad (4)$$

where

$$\mathbf{u}_H = \frac{c_E \cdot \mathbf{u}_E + c_N \cdot \mathbf{u}_N}{\|c_E \cdot \mathbf{u}_E + c_N \cdot \mathbf{u}_N\|} \quad (5)$$

are the unit vectors ($\mathbf{u}_H^a$ or $\mathbf{u}_H^d$), contained in the horizontal plane, perpendicular to the directions of the satellite ground tracks (respectively, ascending and descending); $\mathbf{u}_E$, $\mathbf{u}_N$ are the unit vectors pointing to the east and north directions, respectively; $c_E$ and $c_N$ are constants to be determined by imposing the orthonormality condition of vector $\mathbf{u}_H$ to the satellite ground track; and $\mathbf{u}_Z$ is the unit vector giving the vertical direction, positive when pointing upward. The projection on the LOS direction of 3-D velocity estimated by GPS is given by

$$\mathbf{v}_{GPS} = v_{GPS}^{(E)} \cdot \mathbf{u}_E + v_{GPS}^{(N)} \cdot \mathbf{u}_N + v_{GPS}^{(Z)} \cdot \mathbf{u}_Z. \quad (6)$$

This equation can also be written as

$$\mathbf{v}_{GPS} = v_{GPS}^{(H)} \cdot \mathbf{u}_H + v_{GPS}^{(Z)} \cdot \mathbf{u}_Z \quad (7)$$

with

$$v_{GPS}^{(H)} = \sqrt{v_{GPS}^{(E)}{}^2 + v_{GPS}^{(N)}{}^2}. \quad (8)$$

In the general case, interpolating $v_{GPS}^{(H)}$ over space would not be a sane operation since there could be discontinuities in the terrain displacement pattern. A further problem could be a bad distribution of GPS network over space. However, in many cases, $v_{GPS}^{(H)}$ is quite homogeneous, and the GPS network is well distributed over space. In such cases, $v_{GPS}^{(H)}$ can be safely interpolated to the PS lying in a small neighborhood of a GPS station. A minimum curvature interpolator is used since we are looking for a homogeneous surface. Inserting this interpolated horizontal velocity in (4), the vertical velocity of PS can be retrieved. It is worth noting that, in this way, we avoid to take into account the bias between GPS and PS velocities in both the horizontal and vertical directions. A calibration step is needed since InSAR velocities are not absolute but relative to a reference point in the interferogram. A circular area with a radius $R$ is selected around each GPS station. Then, PS falling within each of those areas are identified, and median vertical velocity is computed. For each set of PS, the interquartile distance is also computed as a measure of dispersion around the median value. This operation is repeated for all GPS stations and for both ascending and descending InSAR time series. The bias function $D$ between GPS and PS-InSAR estimation vertical velocities is computed by minimizing, separately for the ascending and descending passes, the cost function

$$H = \sum_{i=1}^{N_{GPS}} \left\{ \mu \left\{ v_{PS}^{(Z)} \right\}(i) + D(\varphi, \lambda) - v_{GPS}^{(Z)}(i) \right\}^2 \quad (9)$$

where $N_{GPS}$ is the number of GPS stations, $v_{GPS}^{(Z)}(i)$ are the vertical velocities derived from GPS, $\mu\{v_{PS}^{(Z)}\}(i)$ is the median velocity of PS belonging to the 200-m-circular area around the $i$th GPS station, and $D$ is a four-parameter trigonometric polynomial representing a bias and a tilt given by

$$D(\varphi, \lambda) = \alpha \cos \varphi \cdot \cos \lambda + \beta \cos \varphi \cdot sin\lambda + \gamma \sin \varphi + \delta \quad (10)$$

where $\varphi$ and $\lambda$ are the latitude and longitude, respectively, and $(\alpha, \beta, \gamma, \delta)$ are the polynomial coefficients to be estimated by minimizing (9), where $(\alpha, \beta, \gamma)$ are the coordinate differences of the centers of the two ellipsoids to which InSAR and GPS data are referred to, and $\delta$ is a constant bias (see, e.g., [18, p. 213] for details). This operation is performed separately for the ascending and descending PS-InSAR data sets which generally consist of different sets of PSs. The median vertical velocity is used in (10) instead of the mean value since it is less affected by outliers related to noise and/or processing errors. It should be noted that InSAR maps could be affected by long wavelength residual unmodeled errors due to unwrapping, orbital errors, and uncorrected atmospheric artifacts. Observations made by GPS are not expected to have significant systematic errors. The estimated bias and tilts are then removed from the PS estimates, thus obtaining a map of the vertical component of displacement velocity with the same spatial density as the PS-InSAR data set. The map of 3-D velocity can finally be obtained by summing the horizontal component of velocity measured by GPS.

## III. GPS MEASUREMENTS

A dense geodetic network was installed in 2001 in the central group of Azores archipelago (Terceira, Faial, Pico, Graciosa, and S. Jorge islands). It consists of 64 stations distributed
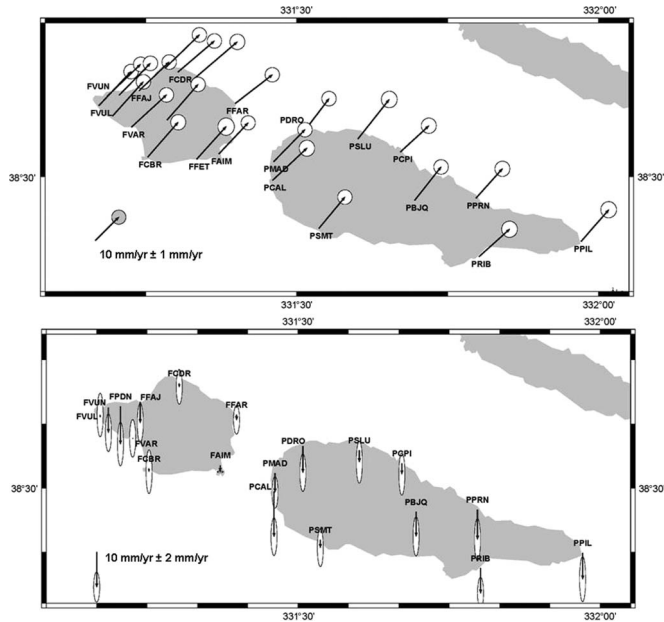
Fig. 2. Terrain displacement velocity measured by GPS in the period 2001–2006. (Top) Horizontal and (bottom) vertical components.

mostly along the coast of the islands. There are 20 stations on Faial island and 12 on Pico island with metallic benchmarks installed in outcrops of solid rock. Four GPS campaigns were conducted from 2001 to 2006 [6]. All the surveys were performed using dual-frequency GPS receivers, collecting data every 30 s. The GPS data analysis has been conducted using the GAMIT and GLOBK software [19], [20] in a three-step approach, described by Feigl *et al.* [21]. GPS data from a few International GPS Service (IGS) and European Reference Frame sites were included in order to serve as ties with the International Terrestrial Reference Frame2000 (ITRF2000) [22]. We used precise satellite orbits computed at the Scripps Orbit and Permanent Array Center at the Scripps Institution of Oceanography [23] from the data collected by the permanent tracking stations of the IGS for geodynamics [24]. The final solution is based on 26 globally distributed stations, which we chose as the ones with the lowest uncertainties in position and velocity in the ITRF2000 definition. The one sigma uncertainties for the GPS velocities of our sites were derived by scaling the formal errors by the square root of chi square per degree of freedom of the final adjustment. The chi square per degree of freedom for this solution was 1.05, indicating a reasonable agreement and a robust estimation of parameters. Fig. 2 depicts the horizontal and vertical velocities of terrain displacement referred to the period 2001–2006. As far as the precisions are concerned, the vertical precision is smaller than $3.0 \text{ mm} \cdot \text{yr}^{-1}$, and the horizontal one is smaller than $1.22 \text{ mm} \cdot \text{yr}^{-1}$ in the north–south direction and $1.15 \text{ mm} \cdot \text{yr}^{-1}$ in the east–west direction. Measurements of the horizontal velocity are characterized by a small dispersion both in speed $(19.0 \pm 1.7 \text{ mm} \cdot \text{year}^{-1})$ and direction in the plane $45.9° \pm 3.8°)$. Vertical velocity, even if smaller in absolute value, is characterized by a much more spatial diversity with faster displacements occurring in the western part of Faial island and along the northern coast of Pico island.

## IV. InSAR Measurement

### A. Data Set and Processing

The interferometric data set consisted of 57 ENVISAT-ASAR images covering Faial and Pico islands, from March 2006 to January 2009. Twenty-nine images were acquired along the descending pass and 28 along the ascending one. The DORIS software (Delft University of Technology, Delft, Netherlands) [25] was used for interferometric processing. The major difficulty in interferometric processing was the coregistration step, due to the minimal amount of land area, and low coherence values related to lush vegetation. Sea pixels were masked in the original data so improving considerably the coregistration and interferometric processing. The interferometric coherence was considerably low, and the PSs approach was the only reliable technique to extract useful information from interferograms. The Stanford Method for PS software [17] was used to determine PS using the stack of interferograms already processed for the two passes. About 350 and 950 PS, respectively, in the ascending and descending passes, were found on the Faial island. A larger number of PS was found on the Pico island: about 2250 in the ascending data set and 1700 in the descending data set. These PS are mostly concentrated on the border of the islands and on a few urban areas with an average density of **5** PS/km$^2$ on both Faial and Pico islands.

### B. Atmospheric Artifact Mitigation

Atmospheric phase delays were calculated using forecasts based on the WRF model and a ray-tracing procedure [16]. Forecasts of atmospherical parameters were generated over a $1 \times 1$ km grid. The initial and time-dependent conditions are derived from the European Centre for Medium Range Weather Forecasts-ERA Interim reanalysis. Simulations were conducted starting 12 h before SAR acquisition time. Delays were interpolated over the geolocated InSAR grid [26]–[28]. Synthetic interferograms corresponding to the atmospheric phase delays were then obtained as the difference between the atmospheric phase delays computed at the acquisition times of the master and slave SAR images. Before applying the PS-InSAR processing, atmospheric artifacts were mitigated by removing the corresponding synthetic interferogram of atmospheric phase delay from each SAR interferogram of the time series.

## V. Data Merging and Quality Assessment

Estimations of terrain displacement velocity made by GPS and InSAR are not directly comparable. In fact, while GPS processing gives absolute velocities referred to a regional or global geodetic reference system (e.g., European Terrestrial Reference System or International Terrestrial Reference System), the InSAR technique can just measure relative velocities with respect to a reference point in the scene. Absolute velocities are recovered if the reference point is known to be at rest or if its displacement velocity is known. To cope with this problem, GPS and InSAR estimations of velocity were processed by means of the methodology described in Section II. First, we should observe that InSAR data and GPS measurements cover
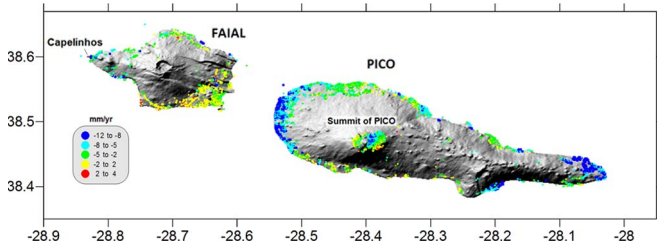
Fig. 3. Map of terrain displacement PS-InSAR vertical velocity overlaid to a shaded relief of Pico and Faial islands. Estimates of both ascending and descending data sets are merged.

different elapsed time intervals. However, terrain displacement at Pico and Faial islands is expected to be mostly smooth in the period 2001–2009 since no large earthquakes have been recorded here during this period. For each GPS station, a circular area with a 200-m radius was selected. This radius value was chosen, based on the knowledge of local geology, to fulfill the hypothesis of homogeneous horizontal velocity, needed to interpolate the GPS velocity at PS positions. PSs, of both ascending and descending data sets, falling within each of those areas, were identified. The horizontal velocity within this area can be considered constant as confirmed by GPS measurements presented in Section III. Furthermore, known tectonic phenomena in these islands do not vary within areas having such a size. It was possible to associate PS to only 14 of the 18 available GPS stations, with the number of PS falling close to a GPS station varying from 4 to 41. The cost function (9) was minimized for each data set, and the parameters of the bias function $D$ were estimated. Fig. 3 displays the integration of vertical terrain velocity estimated by both ascending and descending data sets. Atmospheric effects were mitigated in both data sets. The map in Fig. 3 is spatially consistent and reveals a vast area of vertical displacement on the western and eastern parts of Pico island and on the western part of Faial close to Capelinhos eruption place [29]. A vertical subsidence on the top summit of Pico (with an altitude of 2400 m) is also observed. For each set of PS, both ascending and descending, falling within the circular areas, the interquartile distance as a measure of dispersion of their vertical velocities was computed. It is worth noting that PS velocity does not follow a normal distribution and may contain outliers. Because of these, the interquartile range is more representative than the standard deviation as an estimate of the spread of data, since changes in the upper and lower 25% of the data do not affect it. Fig. 4 reports, for all GPS stations used in this paper, the interquartile range and median velocity of PS and the corresponding GPS measurements of vertical velocity. It was observed that the merging of PS-InSAR and GPS data reduces the velocity dispersion of PS falling within the circular area around each GPS station from 4.6 mm $\cdot$ yr$^{-1}$ to 1.9 mm $\cdot$ yr$^{-1}$ on Faial island, and from 7.2 mm $\cdot$ yr$^{-1}$ to 2.1 mm $\cdot$ yr$^{-1}$ on Pico island. The use of the WRF model further reduces the dispersion of estimates to 1.5 mm $\cdot$ yr$^{-1}$ almost everywhere on both islands. The mitigation of atmospheric artifacts, without the merging of GPS data, reduces the velocity dispersion from 4.6 mm $\cdot$ yr$^{-1}$ to 3.7 mm $\cdot$ yr$^{-1}$ on Faial island, and from 7.2 mm $\cdot$ yr$^{-1}$ to 5.7 mm $\cdot$ yr$^{-1}$ on Pico island. Table I summarizes the dispersion
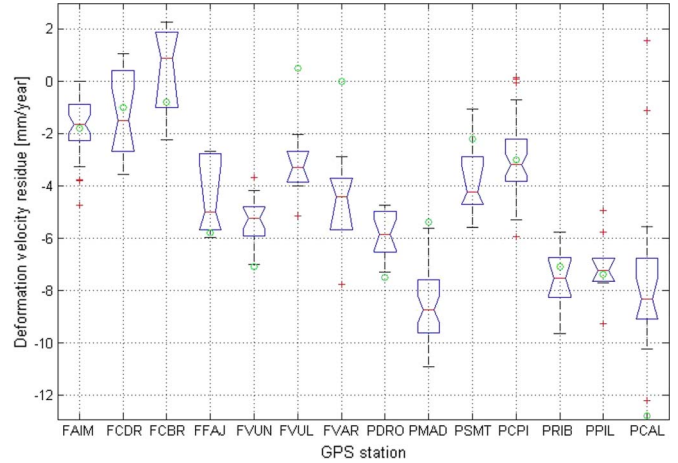


Fig. 4. Box plot of vertical terrain displacement velocity close to the GPS stations. On each box, the central mark is the median, and the edges are the 25th and the 75th percentiles. The whiskers above and below each box extend to the most extreme data points not considered outliers, and outliers are plotted individually as crosses. Circles indicate GPS measurements. For each GPS station, the box plot contains the vertical velocities between the first and third interquartile at PS located within a 200-m distance.

TABLE I
VERTICAL VELOCITY DISPERSION (MILLIMETER/YEAR) OVER THE PICO AND FAIAL ISLANDS AT DIFFERENT PROCESSING STEPS

| Processing | PICO | FAIAL |
|---|---|---|
| PS | 4.6 | 7.2 |
| PS+WRF | 3.7 | 5.7 |
| PS+GPS | 1.9 | 2.1 |
| PS+WRF+GPS | 1.6 | 1.5 |

of PS velocities, quantified in terms of interquartile distance, at each processing step. For all GPS stations, the interquartile range of the PS vertical velocity is lower than the estimated GPS vertical accuracy. For example, at the Faial Instituto Meteorologia (FAIM) GPS station, on the southeastern part of Faial island, 41 PS were selected, and an interquartile range of 1.3 mm $\cdot$ yr$^{-1}$ was determined. The highest interquartile ranges of 3.0 and 2.9 mm $\cdot$ yr$^{-1}$ were observed, respectively, at Faial Castelo Branco (FCBR) (southwestern part of Faial) and Faia Faja (FFAJ) stations and are due to the reduced number of PS close to these stations (only four and six, respectively).

## VI. CONCLUSION

The problem of merging PS-InSAR estimates and repeated GPS measurements of terrain displacement velocity was studied. It was shown that retrieving the 3-D velocity field is difficult and inaccurate due to ill-conditioned matrix bearing the information on the InSAR configuration. Hence, a simple procedure was proposed to extract the 3-D velocity field based on the merging of ascending and descending InSAR data and repeated GPS measurements of terrain displacement velocity. Time series of InSAR images were processed to estimate the LOS components of displacement velocity of PS. The two sets of ascending and descending PS were scanned to identify and label the PS located within a maximum distance

of 200 m around each GPS station. The GPS measurement of the horizontal component at one station was then used to derive the vertical component of velocity at each PS labeled as belonging to the neighborhood of that station. The vertical velocities of the two sets of PS, ascending and descending, were jointly calibrated with the corresponding GPS measurements by minimizing a cost function. The final 3-D velocity map was obtained by adding the horizontal velocity measured by GPS. The accuracy of the 3-D velocity estimation was increased by applying a procedure for the mitigation of atmospheric phase delay based on WRF forecasts. It was observed that the mitigation of atmospheric artifacts reduces the spatial dispersion of velocity estimates up to 30%. The typical requirements to apply this method are the availability of both ascending and descending InSAR data sets, an estimate of atmospheric phase delay at the time of SAR acquisitions, and GPS measurements of terrain displacements. The minimum number of GPS stations depends on the number of parameters needed in the merging procedure.

## References

[1] P. A. Rosen, S. Hensley, I. R. Joughin, F. K. Li, S. N. Madsen, E. Rodriguez, and R. M. Goldstein, "Synthetic aperture radar interferometry," *Proc. IEEE*, vol. 88, no. 3, pp. 333–382, Mar. 2000.

[2] G. Nico, D. Leva, J. Fortuny-Guasch, G. Antonello, and D. Tarchi, "Generation of digital terrain models with a ground-based SAR system," *IEEE Trans. Geosci. Remote Sens.*, vol. 43, no. 1, pp. 45–49, Jan. 2005.

[3] D. Massonnet and K. L. Feigl, "Radar interferometry and its application to changes in the earth's surface," *Rev. Geophys.*, vol. 36, no. 4, pp. 441–500, Nov. 1998.

[4] F. Casu, M. Manzo, A. Pepe, and R. Lanari, "SBAS-DInSAR analysis of very extended areas: First results on a 60000- $km^2$ test site," *IEEE Geosci. Remote Sens. Lett.*, vol. 5, no. 3, pp. 438–442, Jul. 2008.

[5] G. Dalla Via, B. Crippa, E. M. T. Serra, G. Giacomuzzi, and R. Sabadini, "Exploitation of high-density DInSAR data points of the Umbria-Marche (Italy) 1997 seismic sequence for fault characteristics," *Geophys. Res. Lett.*, vol. 34, no. 17, p. L17301, 2007.

[6] C. Catita, K. L. Feigl, J. Catalão, J. M. Miranda, and L. M. Victor, "InSAR time-series analysis of the 9 July Azores earthquake," *Int. J. Remote Sens.*, vol. 26, no. 13, pp. 2715–2729, Jul. 2005.

[7] M. Dehghani, M. J. V. Zoej, I. Entezam, A. Mansourian, and S. Saatchi, "InSAR monitoring of progressive land subsidence in Neyshabour, northeast Iran," *Geophys. J. Int.*, vol. 178, no. 1, pp. 47–56, Jul. 2009.

[8] E. Trasatti, F. Casu, C. Giunchi, S. Pepe, G. Solaro, S. Tagliaventi, P. Berardino, M. Manzo, A. Pepe, G. P. Ricciardi, E. Sansosti, P. Tizzani, G. Zeni, and R. Lanari, "The 2004–2006 uplift episode at Campi-Flegrei caldera (Italy): Constraints from SBAS-DInSAR ENVISAT data and Bayesian source inference," *Geophys. Res. Lett.*, vol. 35, no. 7, p. L07 308, 2008.

[9] F. Catani, P. Farina, S. Moretti, G. Nico, and T. Strozzi, "On the application of SAR interferometry to geomorphological studies: Estimation of landform attributes and mass movements," *Geomorphology*, vol. 66, no. 1–4, pp. 119–131, Mar. 2005.

[10] A. Hooper, P. Segall, and H. Zebker, "Persistent scatterer interferometric synthetic aperture radar for crustal displacement analysis, with application to Volcano Alcedo, Galapagos," *J. Geophys. Res.-Solid Earth*, vol. 112, no. B7, p. B07407, 2007.

[11] S. Gudmundsson and F. Sigmundsson, "Three-dimensional surface motion maps estimated from combined interferometric synthetic aperture radar and GPS data," *J. Geophys. Res.-Solid Earth*, vol. 107, no. B10, p. 2250, 2002.

[12] S. Samsonov and K. Tiampo, "Analytical optimization of a DInSAR and GPS dataset for derivation of three-dimensional surface motion," *IEEE Geosci. Remote Sens. Lett.*, vol. 3, no. 1, pp. 107–111, Jan. 2006.

[13] F. Onn and H. A. Zebker, "Correction for interferometric synthetic aperture radar atmospheric phase artifacts using time series of zenith wet delay observations from a GPS network," *J. Geophys. Res.-Solid Earth*, vol. 111, p. B09102, 2006.

[14] Z. Li, E. J. Fielding, P. Cross, and J. P. Muller, "Interferometric synthetic aperture radar atmospheric correction: Medium Resolution Imaging Spectrometer and Advanced Synthetic Aperture Radar Integration," *Geophys. Res. Lett.*, vol. 33, no. 6, p. L06816, 2006.

[15] J. Foster, B. Brooks, T. Cherubini, C. Shacat, S. Businger, and C. L. Werner, "Mitigating atmospheric noise for InSAR using a high-resolution weather model," *Geophys. Res. Lett.*, vol. 33, p. L16304, 2006.

[16] G. Nico, R. Tomé, J. Catalão, and P. Miranda, "On the use of WRF model for the mitigation of atmospheric effects in InSAR interferograms," *IEEE Trans. Geosci. Remote Sens.*, to be published.

[17] A. Hooper, H. Zebker, P. Segall, and B. Kampes, "A new method for measuring displacement on volcanoes and other natural terrains using InSAR persistent scatterers," *Geophys. Res. Lett.*, vol. 31, no. 23, p. L23611, 2006.

[18] W. A. Heiskanen and H. Moritz, *Physical Geodesy*. San Francisco, CA: Freeman, 1967.

[19] R. King and Y. Bock, "Documentation for the GAMIT GPS software analysis, release 10.05," MIT Cambridge, Atmos., Planet. Sci., Univ. California, San Diego, CA, 2001.

[20] T. A. Herring, "GLOBK: Global Kalman filter VLBI and GPS analysis program," MIT, Cambridge, MA, 2003, Internal Memorandum, ver. 10.1.

[21] K. Feigl, D. Agnew, Y. Bock, D. Dong, A. Donnellan, B. Hager, T. Herring, D. Larsen, K. Larson, M. Murray, Z. Shen, and F. Webb, "Space geodetic measurement of the velocity field of central and southern California, 1984–1992," *J. Geophys. Res.*, vol. 98, no. B12, pp. 21 677–21 712, 1993.

[22] Z. Altamimi, P. Sillard, and C. Boucher, "ITRF2000: A new release of the International Terrestrial Reference Frame for earth science applications," *J. Geophys. Res.*, vol. 107, no. B10, p. 2214, 2002. doi:10.1029/2001JB000561.

[23] P. Fang and Y. Bock, Scripps orbit and permanent array center 1995 report to IGS, International GPS Service for Geodynamics 1995 annual report, pp. 103–124, Pasadena, CA1996.

[24] G. Beutler, I. I. Mueller, and R. E. Neilan, "The International GPS Service for Geodynamics (IGS): Development and start of official service on January 1," *Bull. Geod.*, vol. 68, pp. 39–70, 1994.

[25] B. Kampes, R. Hanssen, and Z. Perski, "Radar interferometry with public domain tools," in *Proc. FRINGE*, Frascati, Italy, Dec. 1–5, 2003.

[26] M. Schwäbisch, "A fast and efficient technique for SAR interferogram geocoding," in *Proc. IEEE IGARSS*, Seattle, WA, 1998, pp. 1100–1102.

[27] G. Nico, "Exact closed-form geolocation of SAR interferometry," *IEEE Trans. Geosci. Remote Sens.*, vol. 40, no. 1, pp. 220–222, Jan. 2002.

[28] E. Sansosti, "A simple and exact solution for the interferometric and stereo SAR geolocation problem," *IEEE Trans. Geosci. Remote Sens.*, vol. 42, no. 8, pp. 1625–1634, Aug. 2004.

[29] J. Catalão, J. M. Miranda, and N. Lourenço, "Deformation associated with the Faial (Capelinhos) 1956 eruption. Inferences from 1937–1997 geodetic measurements," *J. Volcanol. Geotherm. Res.*, vol. 155, no. 3/4, pp. 151–163, Jul. 2006. doi:10.1016/j.jvolgeores.2006.03.028.

**João Catalão** (M'10) was born in Lisbon, Portugal, in 1962. He received the "Licenciatura" degree from the University of Lisbon, Lisbon, in 1986 and the Ph.D. degree in geographic engineering from the University of Lisbon in 1999.

He is currently an Associate Professor with the Department of Geographic Engineering, Geophysics and Energy, University of Lisbon, where he is a Member of the executive council and Coordinator of the Master program. His research is focused on measuring and monitoring the deformation of the Earth's surface using multiple sensors [GPS, synthetic aperture radar (SAR), interferometric synthetic aperture radar, accelerometers, and distance meters]. He is currently working on the tropospheric water vapor mapping using SAR interferometry, GPS, and numerical forecasting models.

**Giovanni Nico** (M'00–SM'06) received the Laurea and Ph.D. degrees in physics from the University of Bari, Bari, Italy, in 1993 and 1999, respectively.

He is currently a Researcher with the Istituto per le Applicazioni del Calcolo, National Research Council (CNR), Bari. He is also an Adjunt Professor of physics with the Università della Basilicata, Matera, Italy. He held visiting positions at the Instituto Dom Luís, Lisbon, Portugal, and the German Remote Sensing Data Center, German Aerospace Center (DLR), Oberpfaffenhofen, Germany. He was a Postdoctoral Fellow at the Joint Research Center, European Commission, and the European Space Agency. His main research interests are in the fields of statistical signal processing, synthetic aperture radar data processing and simulation, spaceborne and ground-based SAR interferometry, and space geodesy.

**Ramon Hanssen**, photograph and biography not available at the time of publication.

**Cristina Catita** received the Ph.D. degree in geographic engineering and geoinformatics from the University of Lisbon, Lisbon, Portugal, in 2008.

Since 1995, she has cooperated with the Faculty of Sciences, University of Lisbon, in the field of geographic engineering. She is currently an Assistant Professor of geographic information systems and spatial analysis of geographic information. From 1995 to 2004, she was a Member of the Tectonophysics and Experimental Tectonics, a Research Unit of the Faculty of Sciences, University of Lisbon, where her main research contribution was in GPS time series analysis and interferometric synthetic aperture radar measurements applied to the study of ground motion deformations. Since 2004, she has been with the Instituto Dom Luís Research Institute, University of Lisbon, as a Member of the GEO-Hazards and Warning Systems group. Her current research interests are in spatial and spatiotemporal data modeling, analysis, and 3-D geovisualization.